Journal of Sea Research 143 (2019) 119–127

Contents lists available at ScienceDirect

Journal of Sea Research

journal homepage: www.elsevier.com/locate/seares

Dynamic Energy Budget theory predicts smaller energy reserves in thyasirid bivalves that harbour symbionts

Joany Mariño[a,*], Starrlight Augustine[b], Suzanne C. Dufour[a], Amy Hurford[a,c]

[a] Department of Biology, Memorial University of Newfoundland, St. John's A1B 3X9, Canada
[b] Akvaplan-niva, Fram High North Research Centre for Climate and the Environment, Tromsø 9296, Norway
[c] Department of Mathematics and Statistics, Memorial University of Newfoundland, St. John's A1C 5S7, Canada

ARTICLE INFO

Keywords:
Chemosymbiosis
Ecophysiology
Mixotrophy
Parathyasira
Thyasira
Seasonality

ABSTRACT

Dynamic Energy Budget (DEB) theory describes the ecophysiology of individuals and distinguishes between the biomass of an organism that functions as an energy reserve and as a structure. DEB theory offers a robust framework to infer and contrast energy allocation patterns, even in data-poor species. We used this approach to compare two thyasirid bivalves that have scarce data: *Thyasira* cf. *gouldi* and *Parathyasira* sp., which co-occur in a seasonal environment, show similar life history features, and are both particulate feeders. However, *T.* cf. *gouldi* hosts chemosymbiotic bacteria that are digested as an additional resource, and how this mixotrophy affects the energy budget of these chemosymbiotic thyasirids is unknown. We used allometric and life history data to parameterize a DEB model for each species and found that symbiotic *T.* cf. *gouldi* has a smaller fraction of its biomass as an energy reserve relative to *Parathyasira*. A smaller energy reserve, in turn, implies reduced energy assimilation and mobilization fluxes, lower somatic maintenance costs and growth rate, and larger energy allocation to maturity and reproduction in symbiotic *T.* cf. *gouldi*. For a thyasirid inhabiting an environment with seasonal forcing, these life history traits may represent an evolutionary strategy where the symbionts function as a partial energy reserve. Our results elucidate a potential role of the chemosymbiotic bacteria in the ecophysiology of a bivalve host, and highlight how the symbiotic association is likely to alter the energy budget of a mixotrophic thyasirid.

1. Introduction

Among symbiotic relationships, the association between chemosynthetic bacteria and invertebrate animals is a prominent example because of its prevalence in diverse marine habitats and within multiple phyla of hosts (Dubilier et al., 2008), especially within the Bivalvia (Roeselers and Newton, 2012). One particular family of bivalves, the Thyasiridae, is notable for containing symbiotic as well as asymbiotic species (Southward, 1986; Taylor et al., 2007). Thyasirids gain nutrients by particulate feeding, with symbiotic and some asymbiotic species likely ingesting free-living, sediment-dwelling chemosynthetic bacteria collected using their elongated foot (Zanzerl and Dufour, 2017). Symbiotic thyasirids, such as *Thyasira* cf. *gouldi*, periodically endocytose and digest symbionts (Dufour et al., 2014), which are harboured extracellularly on gill epithelial cells (Southward, 1986). For the thyasirid host, symbiosis is a trophic interaction where bacterial endosymbionts constitute an additional food source (Dando and Spiro, 1993). However, the thyasirids are still one of the least studied bivalve groups: their taxonomic classification remains uncertain (with many unnamed species), and their symbiotic interaction is poorly understood (Taylor and Glover, 2010). Specifically, the relative importance of chemosymbiosis and particulate feeding (i.e. a mixotrophic diet) in the energy budget of symbiotic thyasirids has yet to be determined.

Representatives of the Thyasiridae are sympatric within the fjord of Bonne Bay (Newfoundland, Canada), an environment that experiences strong seasonal cycles (Laurich et al., 2015). One species, *Parathyasira* sp., is asymbiotic (Batstone et al., 2014). The other taxon resembles *Thyasira gouldi* (in shell characteristics and internal anatomy, hence referred to as *T.* cf. *gouldi*), and forms a complex of cryptic species, which has been provisionally described as three Operational Taxonomic Units (OTUs; Batstone et al., 2014). *T.* cf. *gouldi* displays a unique condition among bivalves that appear to belong to the same species: two of the OTUs are symbiotic and closely related with each other while the third one is asymbiotic (Batstone et al., 2014); here, we focus solely on the symbiotic OTUs 1 and 2. Despite their nutritional differences, *Parathyasira* sp. and symbiotic *T.* cf. *gouldi* (OTUs 1 and 2) share key life

* Corresponding author.
E-mail address: jmarinocoron@mun.ca (J. Mariño).

https://doi.org/10.1016/j.seares.2018.07.015
Received 31 January 2018; Received in revised form 22 July 2018; Accepted 30 July 2018
Available online 07 August 2018
1385-1101/

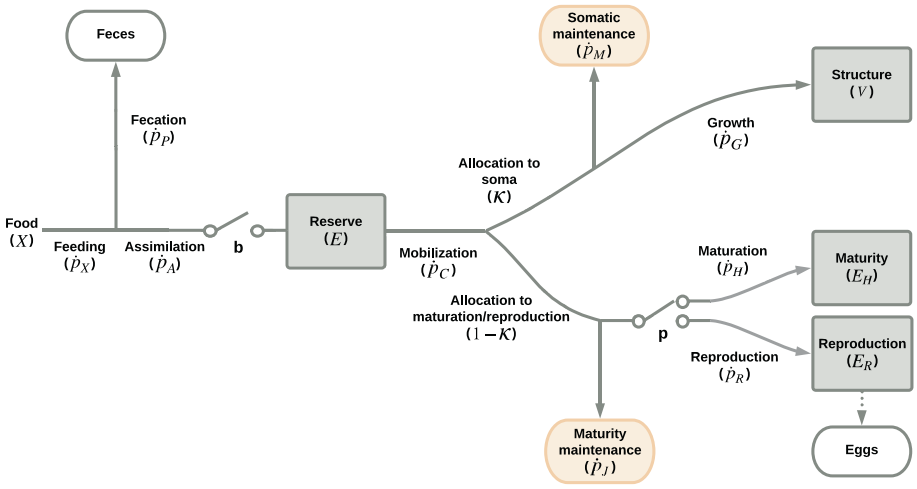

Fig. 1. Schematic representation of the DEB model. Square boxes denote state variables (see Eq. 1), round boxes indicate energy sinks, lines and arrows correspond to the energy fluxes (J/d, see Table 1), dots (˙) indicate rates. The switches **b** and **p** represent metabolic thresholds at birth and puberty, respectively. Food is taken as a forcing variable. See Table 3 for symbol definitions.

Table 1
Energy fluxes (J/d) considered in the DEB-abj model (Kooijman, 2010, 2014). The digestion efficiency from food to reserve is κ_X, κ_P is the fecation efficiency from food to feces, f is the scaled functional response ($0 \leqslant f \leqslant 1$, where 1 is the highest amount of food), $\{\dot{p}_{Am}\}$ is the maximum surface-area specific assimilation rate ($J/d \cdot cm^2$), $\mathscr{M}$ is the metabolic acceleration, $\dot{v}$ is the energy conductance rate from the energy reserve (cm/d), L is the structural length ($L = V^{1/3}$), $\dot{r}$ is the specific growth rate ($1/d$), κ is the fraction of mobilized reserve allocated to soma, $[\dot{p}_M]$ is the volume-specific somatic maintenance cost ($J/d \cdot cm^3$), $\dot{k}_J$ is the maturity maintenance rate coefficient ($1/d$). Notation: square brackets ([]) indicate quantities related to structural volume, curly brackets ({}) denote quantities related to structural surface-area, dots (˙) indicate rates. See DEB-abj model section in the Appendix for definitions.

Flux	Equation
Ingestion/feeding	$\dot{p}_X = \dot{p}_A/\kappa_X$
Fecation	$\dot{p}_P = \kappa_P \dot{p}_X$
Assimilation	$\dot{p}_A = f\{\dot{p}_{Am}\}\mathcal{M}(E_H \geq E_H^b)$
Mobilization	$\dot{p}_C = E(\dot{v}\mathcal{M}/L - \dot{r})$
Allocation to soma	$\kappa \dot{p}_C$
Somatic maintenance	$\dot{p}_M = [\dot{p}_M]L^3$
Growth	$\dot{p}_G = \kappa \dot{p}_C - \dot{p}_M$
Allocation to maturity/reproduction	$(1-\kappa)\dot{p}_C$
Maturity maintenance	$\dot{p}_J = \dot{k}_J E_H$
Maturation	$\dot{p}_H = (1-\kappa)\dot{p}_C - \dot{p}_J$
Reproduction	$\dot{p}_R = (1-\kappa)\dot{p}_C - \dot{k}_J E_H^p$

history traits, particularly puberty and adult sizes (Dufour, 2017), and the role that the symbionts play in the ecophysiology of the host is not clear.

Thyasirids exemplify species in which detailed data are scarce, and in such cases, Dynamic Energy Budget (DEB) theory offers a mechanistic framework to make life history inferences. From general energy partitioning postulates, DEB theory can identify broad metabolic patterns at different stages of an organisms' life cycle. In particular, DEB theory assumes that the energy from food is assimilated into a reserve. A fixed fraction (κ) of the energy reserve is then allocated and used for somatic maintenance and growth, while the rest is invested into maturity maintenance and maturity or reproduction (Fig. 1; Kooijman, 2010). The biomass of the organism is the sum of the masses of reserve and structure; energy invested in maturity and reproduction is assumed to be released into the environment (for complete list of postulates see Table 2.4 in Kooijman, 2010).

The assumptions of DEB theory enable relating simple, measurable quantities (e.g. length at birth, maximum length, length vs. age, weight vs. length) to physiological investment and energy allocation (Kooijman, 2010). For example, an organism that has a large ultimate size also has a high energy assimilation flux and a large energy reserve capacity, relative to a smaller organism of the same species. In this way, we use DEB theory to understand how the thyasirids of Bonne Bay partition their energy. To clarify the underlying effects of mixotrophy in the energy budget of the chemosymbiotic thyasirids, we make quantitative comparisons between the ecophysiological parameters of symbiotic *T.* cf. *gouldi* (OTUs 1 and 2) and *Parathyasira* sp. In this study we focus on elucidating the impact of harbouring symbionts in the life history strategies of *T.* cf. *gouldi*, which may be interpreted as a response to a fluctuating environment.

2. Methods

2.1. DEB-abj model

The individual is represented by four state variables, namely: energy reserve (E, J), volume of structure (V, cm^3), cumulative energy invested into maturation (E_H, J), and cumulative energy invested into reproduction (E_R, J). The dynamic of the individual in time is given by:

$$\begin{aligned} \frac{dE}{dt} &= \dot{p}_A - \dot{p}_C, \\ \frac{dV}{dt} &= \dot{p}_G/[E_G], \\ \frac{dE_H}{dt} &= \dot{p}_H(E_H < E_H^p), \\ \frac{dE_R}{dt} &= \dot{p}_R(E_H = E_H^p), \end{aligned} \quad (1)$$

where $[E_G]$ is the specific cost for structure, E_H^p is the puberty threshold, and $\dot{p}_i$ gives the energy flux of each process i (Table 1).

The cumulative energy invested into maturity (E_H) represents the developmental stage of the organism relative to energy thresholds at developmental milestones (Fig. 2; Augustine, 2017). The first maturity threshold is birth ($E_H = E_H^b$), defined by the beginning of the ingestion of food that is then assimilated into the energy reserve. The next maturity threshold is metamorphosis ($E_H = E_H^j$), because it is assumed that after birth and before puberty there is a different metabolic rate, which results in a temporarily faster growth rate (a pattern termed metabolic or $\mathscr{M}$ acceleration; Kooijman, 2014). The last threshold is puberty ($E_H = E_H^p$), defined as the start of allocation towards reproduction. The puberty threshold is denoted in Eq. 1 by the boolean ($E_H < E_H^p$), defined to have value 1 if true and 0 if false. Once puberty is reached, the cumulative energy invested into reproduction (E_R, or reproduction buffer) is constantly being used in the production of gametes. The DEB-abj model (see details in the Appendix) is a one parameter extension of

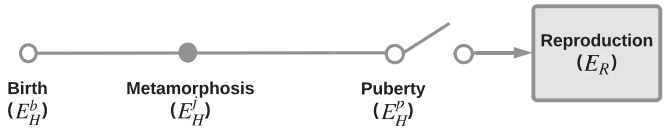

Fig. 2. Life stages in the DEB-abj model are represented by energy thresholds given by the cumulative energy invested in maturity (E_H, Eq. 1). The first threshold is birth ($E_H = E_H{}^b$), defined as the beginning of assimilation from food and the start of metabolic acceleration. The closed circle denotes the metamorphosis threshold, when metabolic acceleration ceases ($E_H = E_H{}^j$). Puberty is the last threshold ($E_H = E_H{}^p$), after which allocation to reproduction starts ($E_H = E_R$).

the standard DEB model, modified to account for the metabolic acceleration, a pattern recognized in bivalves and many other taxa (Kooijman, 2014; Marques et al., 2018a).

2.2. Data

Data are classified as either zero- or uni-variate (Lika et al., 2011a). Zero-variate data are the values of a dependent response variable of the organism at a given time (they constitute single data points, e.g.: length at birth, weight at maximum size). In contrast, uni-variate data consist of values of an independent variable and a dependent response variable (e.g.: length as a function of age, weight as a function of length). In addition to the empirical data from the species, the covariation method used for parameter estimation employs pseudo-data, which act similarly to a prior in Bayesian parameter estimation (Lika et al., 2011a). Pseudo-data are typical, but not species-specific, parameter values from different data sets of a variety of taxa (Table 8.1 Kooijman, 2010; Lika et al., 2011a). These values are not expected to deviate greatly across species, because the magnitude of their variation is restricted by the same physical and chemical constraints that determine the shared metabolic properties of the organisms.

DEB theory treats food and temperature as forcing variables, and assumes that temperature affects all metabolic rates equally (see Section 1.3 in Kooijman, 2010). The model parameters, as well as the empirical and the pseudo-data, are standardized to a reference temperature of 20 °C (T_{ref} = 293.15 K; Lika et al., 2011a). The correction between the reference temperature and the empirical temperature T is done through the Arrhenius relationship (Eq. 1.2 in Kooijman, 2010):

$$c(T) = \exp\left(\frac{T_A}{T_{ref}} - \frac{T_A}{T}\right),$$

where $c(T)$ is the correction factor for a certain temperature T, T_A is the Arrhenius temperature (T_A = 8000 K; Lika et al., 2011a), and T_{ref} is the reference temperature. For example, the reproduction flux (Table 1) at temperature T becomes: $\dot{p}_R(T) = \dot{p}_R(T_{ref})\cdot c(T)$.

Food level is quantified by the scaled functional response f, which can range from no assimilation ($f = 0$) to the highest amount of assimilation ($f = 1$). However, our study focuses on organisms sampled in the field (where individuals were likely to experience a variety of food levels); we do not have precise information on food availability or quality, and how it may change over time. In such cases, the covariation method assumes that food is abundantly available ($f = 1$ for all data sets; Lika et al., 2014). This should be taken as a reference value from which we can compare growth between species (assuming they are subject to the same food availability) as well as between sites in the future (e.g. Ballesta-Artero et al., 2018, this special issue). Further, we assumed that the organism was in equilibrium with the environment, meaning that the reserve density is constant: $d[E]/dt = 0$. These assumptions are included in the covariation method, as they simplify the estimation procedure and allow estimating parameters for species with limited available data (Lika et al., 2014).

The data sets used for both species, including empirical and pseudo-data, are summarized in Table 2. We took the maximum reproductive rate as being equal to that of *Thyasira gouldi*, a closely related species similar in size and habitat (Blacknell, 1973). For the thyasirids collected in Bonne Bay we assumed a body temperature equal to that of the sediment, T = 6 °C (which represents the yearly average; Laurich et al., 2015). For the validation data of *Thyasira gouldi* we set T = 10 °C, after Blacknell (1973). Details regarding data measurements are presented in the Data collection section of the Appendix.

Table 2
Data sets considered in the parameterization and validation of the DEB-abj model. The first row section corresponds to empirical zero- and uni-variate data from the symbiotic *Thyasira* cf. *gouldi* and the asymbiotic *Parathyasira* sp. The second row section indicates uni-variate validation data from *Thyasira gouldi*. The last row section shows the pseudo-data, as specified by the covariation method (Lika et al., 2011a, 2011b). Notation: square brackets ([]) indicate quantities related to structural volume, dots (·) denote rates. See Data collection section of the Appendix for details on measurements.

Symbol	Unit	Description
a_m	d	Life span[a]
L_b	cm	Length at birth[b]
L_p	cm	Length at puberty[c]
L_i	cm	Ultimate total length[d]
Wd_i	g	Ultimate ash-free dry weight
$\dot{R}_m$	$\#/d$	Maximum reproduction rate
tL	d	Length as a function of time
LW_d	–	Ash-free dry weight as a function of length
LN	# eggs	Fecundity as a function of size
TJO	ml/h	Respiration as a function of temperature
WTO	ml/h	Respiration as a function of weight
$\dot{v}$	cm/d	Energy conductance
κ	–	Allocation fraction to soma
$[\dot{p}_M]$	$(J/d \cdot cm^3)$	Volume-specific somatic maintenance cost
κ_G	–	Growth efficiency
$\dot{k}_J$	$1/d$	Maturity maintenance coefficient
κ_R	–	Reproduction efficiency

[a] Average number of annuli in the adult shell.
[b] Length (maximal dimension) of the larval shell.
[c] Size of the smallest individuals seen to bear eggs.
[d] Size of the largest individuals recorded.

2.3. Parameter estimation and measure of fit

To fit the model and estimate the primary parameters, we used an improved version of the covariation method, described in Marques et al. (2018a) and provided in the free and open-source software DEBtool v2017 (Lika et al., 2011a, 2011b), implemented in Matlab (The MathWorks Inc., 2017). This approach takes advantage of the known covariation patterns in the parameters of the DEB model across species and, together with auxiliary theory that links the data to the variables, specifies the mapping functions between the data and the parameter space (Lika et al., 2011a, 2011b, 2014). In this way, all the parameters of the model are estimated simultaneously by fitting the model to the empirical and pseudo-data sets. The estimation consists of simultaneously minimizing the deviation of the model from the data through the Nelder-Mead simplex method (Marques et al., 2018b). Formally, the objective function to be minimized is:

$$\sum_{i=1}^{n}\sum_{j=1}^{n_i} w_{i,j}\frac{(\hat{Y}_{i,j} - Y_{i,j})^2}{\overline{Y}_i^2 + \overline{\hat{Y}}_i^2},$$

where $Y_{i,j}$ is the data indexed by data set, i, and by points within that data set, j. The respective estimate (prediction) of the model is $\hat{Y}_{i,j}$, and $w_{i,j}$ is the weight coefficient. The mean of all data points ($Y_{i,j}$) across the data set i is $\overline{Y}_i$, and the mean of all predictions ($\hat{Y}_{i,j}$) is $\overline{\hat{Y}}_i$. The number of points within the data set i is n_i, and n is the total number of data sets.

The goodness of fit of the model for each data set i is assessed by the relative error (RE). The overall goodness of fit of the model to the data

Table 3
Definitions of the compound parameters and implied properties calculated from the primary parameters of the DEB-abj model (Eq. 1) for the symbiotic *Thyasira* cf. *gouldi* and the asymbiotic *Parathyasira* sp. The maximum surface-area specific assimilation rate is $\{\dot{p}_{Am}\}$ ($J/d \cdot cm^2$), $\dot{v}$ is the energy conductance rate from the energy reserve (cm/d), $[E_G]$ is the volume-specific cost for structure ($J/d \cdot cm^3$), κ is the fraction of mobilized reserve allocated to soma, $[\dot{p}_M]$ is the volume-specific somatic maintenance cost ($J/d \cdot cm^3$), $\dot{k}_J$ is the maturity maintenance rate coefficient ($1/d$). At equilibrium ($d[E]/dt = 0$) $e = f$. Implied properties are evaluated at $f = 1$. Notation: square brackets ([]) indicate quantities related to structural volume, curly brackets ({}) denote quantities related to structural surface-area, dots ($\cdot$) indicate rates.

Symbol	Unit	Description	Definition	Reference
$[E_m]$	J/cm^3	Maximum reserve density	$\{\dot{p}_{Am}\}/\dot{v}$	Table 3.3, Kooijman, 2010
e	–	Scaled energy density	$[E]/[E_m]$	p. 473, Kooijman, 2010
$\dot{k}_M$	$1/d$	Somatic maintenance coefficient	$[\dot{p}_M]/[E_G]$	Table 3.3, Kooijman, 2010
k	–	Maintenance ratio	$\dot{k}_J/\dot{k}_M$	p. 47, Kooijman, 2010
g	–	Energy investment ratio	$[E_G]\dot{v}/(\kappa\{\dot{p}_{Am}\})$	Table 3.3, Kooijman, 2010
$\dot{r}_B$	$1/d$	von Bertalanffy growth rate	$\frac{\dot{k}_M g}{3(e+g)}$	p. 59, Kooijman, 2010
E_0	J	Energy reserve in embryo	Eq. 2.42	Kooijman, 2010
N_i	#	Lifetime reproductive output	$\max\left(0, \frac{\kappa_R \dot{p}_R}{E_0}\right)$	Eq. 2.56, Kooijman, 2010
Wd_0	g	Ash-free dry weight of an embryo	Eq. 3.3	Kooijman, 2010
Wd_{N0}	g	Weight of lifetime reproductive output	$N_i \cdot Wd_0$	
a_i	d	Age at each developmental threshold i		

of each species is measured by the mean relative error ($MRE \in [0, \infty)$) and by the symmetric mean squared error ($SMSE \in [0, 1]$). For all cases, error values of 0 indicate an exact match between the predictions of the model and the data. Details on the approach are given in the Parameter estimation section in the Appendix.

Using the estimated primary parameters of the model we calculated compound parameters (i.e. simple functions of primary parameters) and implied properties (quantities which also depend on food). All quantities were computed for ad libitum food at the typical temperature of 6 °C (Table 3).

2.4. Model validation

Once the parameters of the model were estimated, we validated its predictions with data from *Thyasira gouldi* (Blacknell and Ansell, 1974). These data were chosen as validation because they constitute the only quantitative record of the physiology of thyasirids, obtained under controlled laboratory conditions and at different temperatures. However, these complementary data were excluded from the parameterization (setting a weight coefficient equal to zero) because, although closely related, the measurements correspond to a different species. We digitized these data sets through WebPlotDigitizer (Rohatgi, 2017), and they are presented in Table 2.

2.5. Interspecific comparison of the parameters

In order to quantify the differences between *T.* cf. *gouldi* and *Parathyasira* (considered as the reference species), for each estimated parameter or implied property $\hat{\theta}$ we defined the following relative difference:

$$\rho = \frac{\hat{\theta}_{Thyasira} - \hat{\theta}_{Parathyasira}}{\hat{\theta}_{Parathyasira}}, \quad (2)$$

where $\hat{\theta}_{Thyasira}$ is the value of the parameter or implied property for *T.* cf. *gouldi*, and $\hat{\theta}_{Parathyasira}$ is the value of the corresponding parameter or implied property for *Parathyasira*. According to our formulation, $\rho > 0$ indicates a greater value of the parameter or implied property for *T.* cf. *gouldi* with respect to *Parathyasira* sp., while, $\rho < 0$ indicates a lower quantify for *T.* cf. *gouldi*.

3. Results

3.1. Data, model fit, and validation

The completeness of the data that we compiled is 1.5 (according to the criteria defined by Lika et al., 2011a, which range from a minimum

Table 4
Data and model fit for the symbiotic *Thyasira* cf. *gouldi* and the asymbiotic *Parathyasira* sp. Estimation was performed assuming the reference condition of $f = 1$. The first row section corresponds to empirical zero- and uni-variate data, and the second row section indicates the pseudo-data, which are given for the reference temperature of 20 °C. The fit of the model to each data set is measured by the Relative Error (RE). The last row section indicates the overall fit, quantified by the Mean Relative Error ($MRE \in [0, \infty)$) and the Symmetric Mean Squared Error ($SMSE \in [0, 1]$). In all cases, values of error close to zero indicate a good fit of the model to the data. The reference column indicates the source of the data. Notation: square brackets ([]) indicate quantities related to structural volume, dots (˙) denote rates. See Table 2 for symbol definitions.

	Thyasira cf. *gouldi*			*Parathyasira* sp.			
Symbol	Data	Prediction	RE	Data	Prediction	RE	Reference
a_m	2190	2190	4.633×10^{-8}	2190	2186	0.002	This study
L_b	0.018	0.019	0.004	0.014	0.014	0.002	Giolland and Dufour, 2015
L_p	0.28	0.28	2.942×10^{-4}	0.28	0.28	0.001	Dufour, 2017
L_i	0.514	0.534	0.039	0.514	0.488	0.05	Dufour, 2017
Wd_i	0.002	0.002	0.02	0.003	0.003	0.045	This study
$\dot{R}_m$	6.137	6.145	0.001	6.137	6.105	0.005	Blacknell and Ansell, 1974
tL	Fig. 3		0.028	Fig. 3		0.087	This study
LW_d	Fig. 3		0.33	Fig. 3		0.338	This study
$\dot{v}$	0.02	0.02	0.004	0.02	0.02	0.013	Lika et al., 2011a
κ	0.8	0.882	0.103	0.8	0.958	0.197	Lika et al., 2011a
$[\dot{p}_M]$	18	15.78	0.124	18	23.61	0.312	Lika et al., 2011a
κ_G	0.8	0.8	6.495×10^{-4}	0.8	0.802	0.002	Lika et al., 2011a
$\dot{k}_J$	0.002	0.002	0	0.002	0.002	0	Lika et al., 2011a
κ_R	0.95	0.95	0	0.95	0.95	0	Lika et al., 2011a
MRE			0.053			0.066	
SMSE			0.111			0.116	

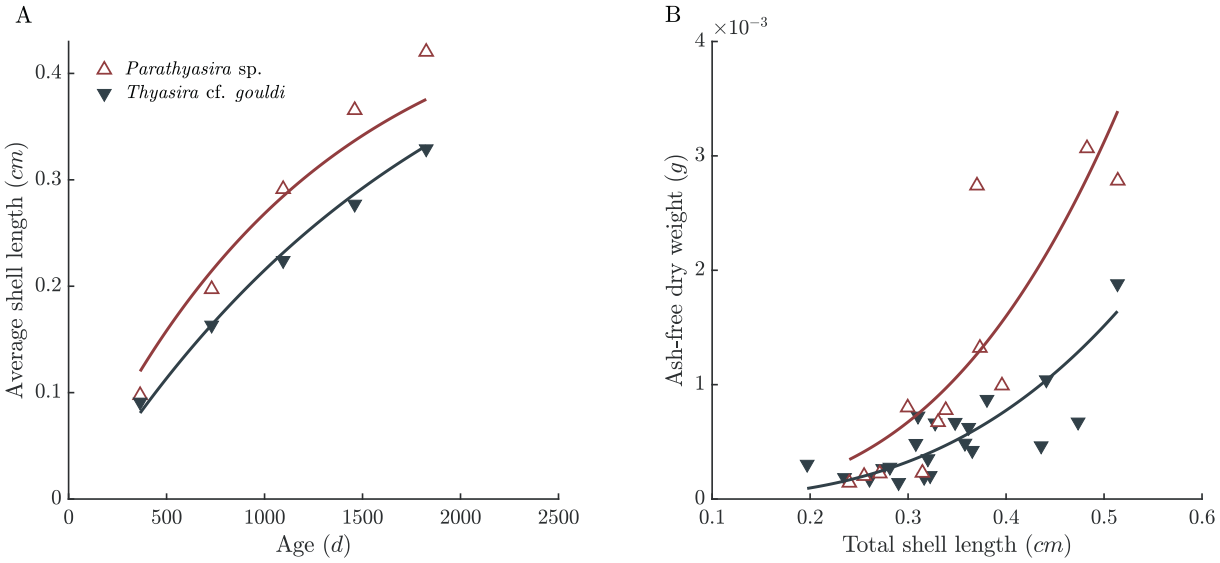

Fig. 3. Uni-variate data (triangles) and model fit (lines) for the symbiotic *Thyasira* cf. *gouldi* and the asymbiotic *Parathyasira* sp. Estimation was performed assuming reference conditions of $f = 1$ and $T = 20$ °C. (A) Average shell length growth (*cm*) in time (*d*) for *T.* cf. *gouldi* ($RE = 0.028$), and *Parathyasira* ($RE = 0.087$). (B) Ash-free dry mass (*g*) as a function of length (*cm*) for *T.* cf. *gouldi* ($RE = 0.33$), and *Parathyasira* ($RE = 0.338$). Both figures show a good fit of the model to the data, particularly for *T.* cf. *gouldi*, as indicated by values of the Relative Error (*RE*) close to zero.

of 0 to a maximum of 10), both for *T.* cf. *gouldi* as well as for *Parathyasira* sp. This level corresponds to data on lengths and weights at specific developmental stages, mean life span, weight as a function of length, and growth in time; which together comprise 7 empirical data sets for each species (Table 4). The fit of the model is consistent with the available data for both thyasirids, as indicated by values of the MRE and the SMSE close to zero (Table 4, Fig. 3). Overall, the fit of the model is more accurate for *T.* cf. *gouldi*.

The predictions of the fitted model for respiration and fecundity agree with the validation data of *Thyasira gouldi* (Table 5, Fig. 4). Model predictions concerning the fecundity and the respiration per gram of dry weight fit better for *T.* cf. *gouldi* than for *Parathyasira* (Fig. 4A, B). However, the predictions regarding respiration as a function of dry weight at different temperatures fit better for *Parathyasira* (Fig. 4C, D).

3.2. Model parameters

Despite of the limited amount of available data, we were able to estimate the values of ten primary parameters of the model for each of the species. The estimated primary parameters are presented in Table 6, and the resulting compound parameters and implied properties in Table 7. The relative difference for each parameter or implied property between *T.* cf. *gouldi* and *Parathyasira* (ρ, Eq. 2) is shown in Fig. 5.

The symbiotic *T.* cf. *gouldi* has a greater fraction of structural biomass (δ_V), which corresponds to a lower fraction of energy reserve (E) and a lower maximum reserve capacity ($[E_m]$) when compared to *Parathyasira* (Table 7, Fig. 5B). The rates of assimilation $\{\dot{p}_{Am}\}$ and somatic maintenance $[\dot{p}_M]$ are also lower for *T.* cf. *gouldi* (Table 6, Fig. 5A). The energy conductance rate ($\dot{v}$) and the specific costs for structure ($[E_G]$) do not differ greatly between the two thyasirids (Table 6, Fig. 5A).

The allocation of reserve energy towards somatic maintenance and growth (κ), is lower for *T.* cf. *gouldi* in comparison to the asymbiotic *Parathyasira* (Table 6, Fig. 5A). Consequently, the fraction allocated towards maturity maintenance and maturation/reproduction ($1 - \kappa$) is greater in *T.* cf. *gouldi*, and the initial reserve present in the embryo is also higher (E_0, Table 3). This suggests larger embryos in the symbiotic thyasirid, as indicated by their estimated weight (Wd_0). Yet, the weight of all the eggs produced in the life time is comparatively less relative to *Parathyasira*, due to fewer embryos being produced (Wd_{N0} and N_i; Table 7, Fig. 5B).

A greater initial energy reserve is reflected in the energy invested into maturity at each developmental stage (E_H^b, E_H^j, E_H^p, Table 6), and in the ages at which they are reached (a_b, a_j, a_p, Table 7), all of which are greater for *T.* cf. *gouldi* relative to *Parathyasira* (Fig. 5A). This means that the symbiotic *T.* cf. *gouldi* requires greater amounts of energy and more time to reach the same developmental thresholds (Fig. 6). The growth rate, measured by the von Bertalanffy growth rate ($\dot{r}_B$), is also lower for *T.* cf. *gouldi* with respect to *Parathyasira* (Table 3, Figs. 3A, 5B).

The main ecophysiological traits linked to the presence of chemoautotrophic symbionts in thyasirid hosts are summarized in Table 8.

Table 5
Validation data and model predictions for the symbiotic *Thyasira* cf. *gouldi*, the asymbiotic *Parathyasira* sp., and *Thyasira gouldi*. Estimation was performed assuming the reference condition of $f = 1$. The fit of the model to each data set is measured by the Relative Error (*RE*). The last row section indicates the overall fit, quantified by the Mean Relative Error ($MRE \in [0, \infty)$) and the Symmetric Mean Squared Error ($SMSE \in [0, 1]$). In all cases, values of error close to zero indicate a good fit of the model to the data. The reference column indicates the source of the data. See Table 2 for symbol definitions.

	Thyasira cf. *gouldi*		*Parathyasira* sp.		
Symbol	Data and prediction	RE	Data and prediction	RE	Reference
LN	Fig. 4A	0.534	Fig. 4A	1.051	Blacknell, 1973
TJO	Fig. 4B	0.192	Fig. 4B	0.596	Blacknell, 1973
*WJO*5	Fig. 4C	0.426	Fig. 4D	1.072	Blacknell, 1973
*WJO*10	Fig. 4C	0.522	Fig. 4D	0.323	Blacknell, 1973
*WJO*15	Fig. 4C	0.241	Fig. 4D	0.221	Blacknell, 1973
MRE		0.182		0.299	
SMSE		0.263		0.279	

4. Discussion

The parameterization of the DEB model for both species predicts that symbiotic *T.* cf. *gouldi* has a smaller fraction of energy reserves relative to *Parathyasira*. A smaller energy reserve in turn implies differences in energy allocation throughout the life history of *T.* cf. *gouldi* (see Table 8). Taking into account the habitat of the thyasirids, these

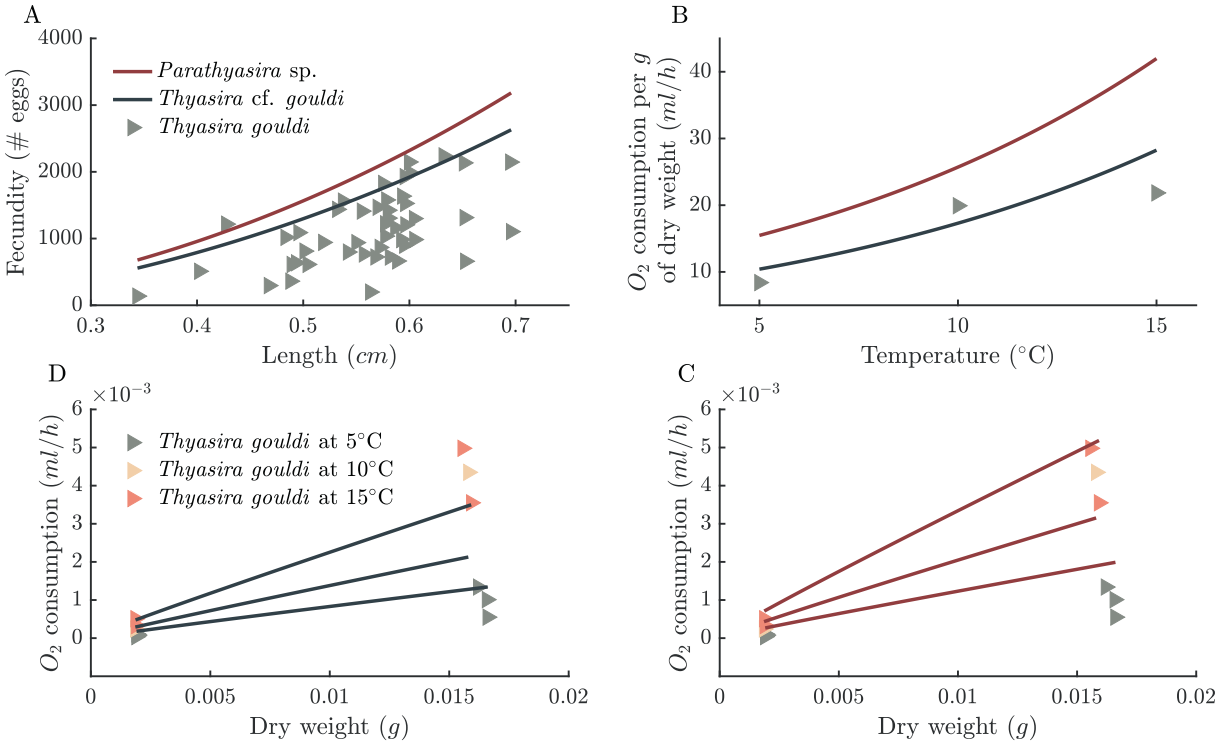

Fig. 4. Uni-variate *Thyasira gouldi* validation data (triangles) and model predictions (lines) for the symbiotic *Thyasira* cf. *gouldi* and the asymbiotic *Parathyasira* sp. The estimation was performed assuming reference conditions of $f = 1$ and $T = 20$ °C. (A) Fecundity (# eggs) as a function of shell length (*cm*) for *T.* cf. *gouldi* (*RE* = 0.534), and *Parathyasira* (*RE* = 1.051). (B) Oxygen consumption (*ml/h*) for 1 *g* of dry weight as a function of temperature for *T.* cf. *gouldi* (*RE* = 0.192), and *Parathyasira* (*RE* = 0.596). (C, D) Oxygen consumption (*ml/h*) as a function of dry weight (*g*) at different temperatures (°C): (C) for *T.* cf. *gouldi* at 5 (*RE* = 0.426), 10 (*RE* = 0.522) and 15 (*RE* = 0.241), and (D) for *Parathyasira* at 5 (*RE* = 1.072), 10 (*RE* = 0.323) and 15 (*RE* = 0.221). Despite of the limited available data for validation, the figures and the values of the Relative Error (*RE*) close to zero show that the model predictions and the validation data agree.

Table 6
Primary parameter estimates of the DEB-abj model (Eq. 1) for the symbiotic *Thyasira* cf. *gouldi* and the asymbiotic *Parathyasira* sp. Rates were calculated at $T = 20$ °C. Notation: square brackets ([]) indicate quantities related to structural volume, curly brackets ({}) denote quantities related to structural surface-area, dots (˙) indicate rates.

Symbol	*Thyasira* cf. *gouldi*	*Parathyasira* sp.	Unit	Description
$\{\dot{p}_{Am}\}$	1.427	2.547	$J/d \cdot cm^2$	Maximum surface-area assimilation rate
$\dot{v}$	0.02	0.02	cm/d	Energy conductance rate
κ	0.883	0.958	–	Allocation fraction to soma
$[\dot{p}_M]$	15.78	23.61	$J/d \cdot cm^3$	Volume-specific somatic maintenance cost
$[E_G]$	2355	2348	J/cm^3	Specific cost for structure
E_H^b	2.639×10^{-4}	7.193×10^{-5}	J	Maturity at birth
E_H^j	0.011	0.002	J	Maturity at metamorphosis
E_H^p	1.283	0.96	J	Maturity at puberty
$\dot{h}_a$	9.844×10^{-4}	1.262×10^{-7}	$1/d^2$	Weibull aging acceleration
δ_M	0.507	0.64	–	Shape coefficient

Table 7
Compound parameters and implied properties of the DEB-abj model (Eq. 1) for the symbiotic *Thyasira* cf. *gouldi* and the asymbiotic *Parathyasira* sp. All of the quantities were calculated at $f = 1$ and $T = 6$ °C. Notation: square brackets ([]) indicate quantities related to structural volume, dots (˙) denote rates. See Table 3 for symbol definitions.

Symbol	*Thyasira* cf. *gouldi*	*Parathyasira* sp.	Unit	Description
δ_V	0.967	0.943	–	Fraction of weight that is structure
$[E_m]$	71.585	125.662	J/cm^3	Maximum reserve capacity
$\dot{k}_M$	0.007	0.01	$1/d$	Somatic maintenance rate coefficient
$\dot{r}_B$	5.535×10^{-4}	8.113×10^{-4}	$1/d$	von Bertalanffy growth rate
g	37.287	19.514	–	Energy investment ratio
k	0.3	0.2	–	Maintenance ratio
a_b	11.625	9.662	d	Age at birth
a_j	306.811	136.823	d	Age at metamorphosis
a_p	1423.35	1075.13	d	Age at puberty
N_i	1.065×10^3	2.214×10^3	#	Lifetime reproductive output
Wd_0	1.003×10^{-7}	7.742×10^{-8}	g	Dry weight of embryo
Wd_{N0}	1.068×10^{-4}	1.715×10^{-4}	g	Dry weight of total lifetime reproductive output
E_0	2.308×10^{-3}	1.782×10^{-3}	J	Energy reserve in embryo
z	0.08	0.103	–	Zoom factor

features may suggest an adaptative strategy in response to a fluctuating resource availability, where the symbionts are likely to function as a partial energy reserve for the host.

4.1. Structure and energy reserve biomass

We found that symbiotic *T.* cf. *gouldi* has a greater proportion of structural biomass relative to *Parathyasira* (Table 7, Fig. 5): this finding has two potential explanations. First, an increased structural volume likely corresponds to the enlarged gills of *T.* cf. *gouldi*, which constitute an adaptation to harbour bacterial symbionts (Dufour, 2005), and so

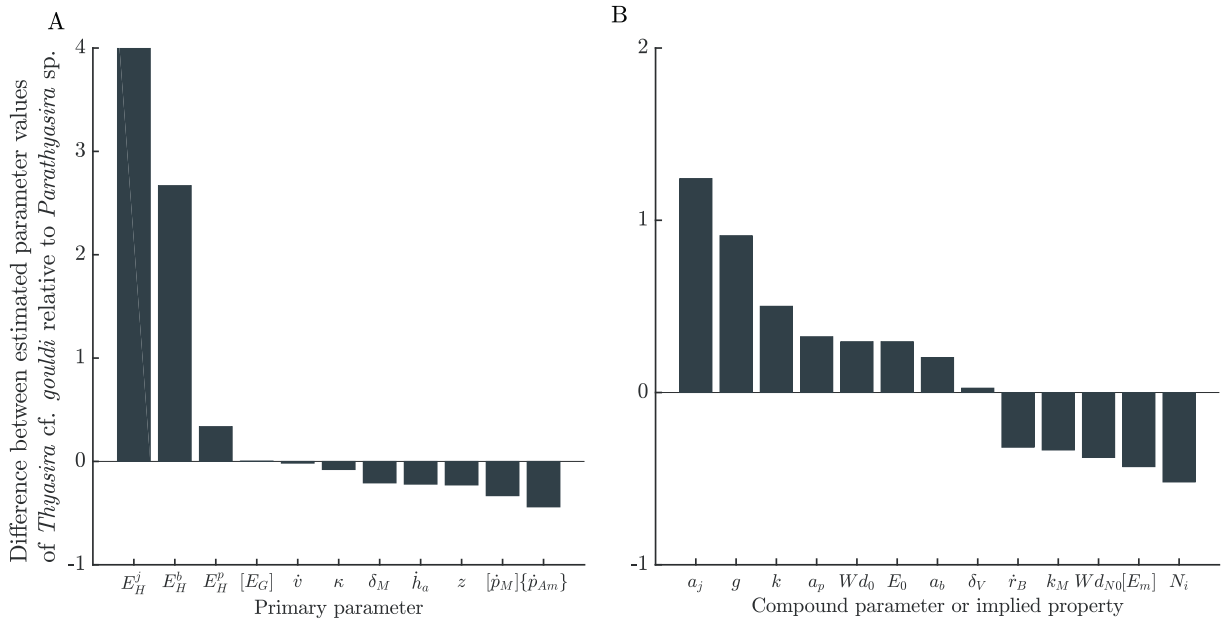

Fig. 5. Relative difference (ρ, Eq. 2) between the estimated values of primary parameters (A, Table 6), compound parameters and implied properties (B, Table 3) of the DEB-abj model (Eq. 1) for the symbiotic *Thyasira* cf. *gouldi* relative to the asymbiotic *Parathyasira* sp. Values above 0 are greater for *T.* cf. *gouldi* relative to *Parathyasira*, while values below 0 are lower for *T.* cf. *gouldi*. The cumulative maturity energy thresholds of life history transitions ($E_H{}^b$, $E_H{}^j$, and $E_H{}^p$), the ages at each stage transition (a_b, a_j, and a_p), the fraction of adult weight that is structure (δ_V), and the embryo weight (Wd_0) are greater for *T.* cf. *gouldi*. The somatic maintenance cost ($[\dot{p}_M]$), reserve capacity ($[E_m]$), maximum assimilation rate ($\{\dot{p}_{Am}\}$), von Bertalanffy growth rate ($\dot{r}_B$), and the lifetime weight of the reproductive output (Wd_{N0}) are all lower for *T.* cf. *gouldi* with respect to *Parathyasira*. See Tables 3, 6, and 7 for notation and definitions.

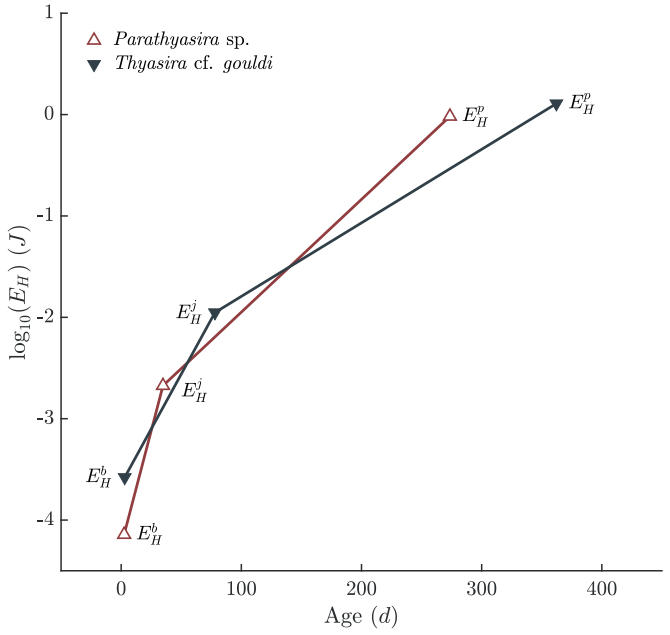

Fig. 6. Log-transformed cumulative energy at birth ($E_H{}^b$, *J*), metamorphosis ($E_H{}^j$, *J*), and puberty ($E_H{}^p$, *J*) for the symbiotic *Thyasira* cf. *gouldi* and the asymbiotic *Parathyasira* sp. as a function of age (*d*). All maturity thresholds and ages are higher for *T.* cf. *gouldi*, indicating a slower development relative to *Parathyasira*. The cumulative energy at puberty is similar for both species, although *T.* cf. *gouldi* needs more time to reach this threshold (Tables 3, 6).

less of *T.* cf. *gouldi* biomass is storage due to the relatively larger structural volume. Second, a greater proportion of structure also implies lower energy reserves for *T.* cf. *gouldi*. Considering that the abundance, uptake, and digestion of the bacterial symbionts show a cyclical trend (Laurich et al., 2015), a low energy reserve suggests that the symbionts may buffer resource fluctuations. For the thyasirids,

Table 8
Summary of the life history traits of the symbiotic *Thyasira* cf. *gouldi* relative to the asymbiotic *Parathyasira* sp., as evidenced by the estimated parameters of the DEB-abj model for each species.

Feature	Reference
Biomass composed of a greater proportion of structure and less of energy reserve.	Table 7
Lower assimilation flux and somatic maintenance cost.	Table 6, Fig. 5A
Lower proportion of energy allocated to somatic mainte- nance and growth; greater proportion allocated towards maturity maintenance and maturation or maturity.	Table 6
Greater cumulative energy thresholds and ages, at birth, metamorphosis, and puberty.	Tables 6, 7, Fig. 6
Lower growth rate.	Table 7, Fig. 6
Greater weight of eggs but lower weight of total embryos, due to production of lower number of embryos.	Table 7, Fig. 5B

reserves would be of particular importance given that they combine foraging on particulate organic matter and on sulfur-oxidizing bacteria from the sediment, both of which are subject to seasonal variations (Dufour and Felbeck, 2003; Dufour et al., 2014). Evidence of this is the larger energy reserve present in the asymbiotic *Parathyasira*, which may represent an adaptation in response to variable food availability. The evolution of an energy reserve has been shown to be an evolutionary stable strategy in fluctuating environments, and at ecological time scales both strategies, with and without energy reserve, can coexist (Kooi and Troost, 2006).

Relating the state variables of the DEB model to measurable components of individuals would provide a test of our hypothesis describing the potential function of symbionts in thyasirids. Specifically, the biochemical estimation of the amount of energy reserves could be achieved by quantifying glycogen or lipid levels. However, due to the small size of the thyasirids, most analyses have to be done combining samples in bulk, which make it difficult to discriminate between the reserve compounds present in different tissues.

4.2. Assimilation, mobilization, allocation to soma and somatic maintenance

Our results indicate that the fraction of energy allocated to somatic maintenance and growth is lower in *T.* cf. *gouldi*, relative to *Parathyasira* (Table 6, Fig. 5A). A lower investment in somatic maintenance and growth is consistent with our explanation of the likely role of the symbionts in averaging resource availability when other sources of food are rare: in species that rely on constant resources, such an allocation pattern has been proposed as an adaptation to reduce the minimum resources required by reducing ultimate size (Kooijman, 2010). However, for *T.* cf. *gouldi* there does not appear to be a reduction in ultimate size, but rather a reduction in growth rate.

The amount of energy reserve in the organism is directly linked to the fluxes of assimilation and mobilization, as well as to the density of the energy reserve itself (Eq. 1, Table 1). A lower amount of energy reserve in symbiotic *T.* cf. *gouldi* indicates that the assimilation flux is also low, as it is shown by the maximum assimilation rate (Table 6, Fig. 5A). Hence, although *T.* cf. *gouldi* may have a constant resource availability, since the symbionts decrease the energy reserve density, the host would be able to sustain a low assimilation rate. The mobilization flux depends on the energy reserve density and on the structural volume (Table 1); consequently —and even with similar conductance rates—, the symbiotic *T.* cf. *gouldi* would have a lower mobilization flux relative to *Parathyasira* (Table 6, Fig. 5A). Both findings signify that *T.* cf. *gouldi* has a lower ratio of assimilation to mobilization flux compared to *Parathyasira*.

The estimated value of the somatic maintenance cost for *T.* cf. *gouldi* is lower relative to *Parathyasira* (Table 6, Fig. 5A), which agrees with the likely role of the bacterial symbionts in buffering resource seasonality. Constant resource availability may allow the host to minimize a possible 'waste' of energy reserve in somatic maintenance (Kooijman, 2013), while being able to attain a similar size and reproductive output than the asymbiotic *Parathyasira*. The significance of the values of somatic maintenance are better understood by contrasting them with those of other taxa. In order to make comparisons, the somatic maintenance must be corrected by their specific density: $[\dot{p}_M]/d_V$ (for $d_V = 0.09$ in bivalves). This correction yields costs of $175.3\, J/g \cdot d$ for the symbiotic *T.* cf. *gouldi*, and $262.3\, J/g \cdot d$ for *Parathyasira*, while the mean value across the bivalves is $255.1\, J/g \cdot d$, and the typical value across all taxa is $200\, J/g \cdot d$. This way, the somatic maintenance for *T.* cf. *gouldi* is also lower relative to the average cost across bivalves and to the typical animal. This finding coincides with the pattern exhibited by the photosymbiotic, tropical bivalve *Tridacna gigas*, which shows the lowest somatic maintenance cost among the bivalves modeled using the DEB framework ($[\dot{p}_M]/d_V = 5.4\, J/d \cdot cm^3$), despite being orders of magnitude higher in size (137 *cm* in length, and 2000 *g* in weight; AmP, 2017). Differences in the physiology and habitat of this unrelated species constrain such a direct comparison; however, the broad similarity in the somatic maintenance may give a general insight into a plausible consequence of harbouring symbionts in the overall energy partitioning of a bivalve host.

The most informative experiments, in terms of data that can be used to parameterize the DEB model, would be those in which growth, reproduction, and respiration are determined simultaneously under different resource conditions (Lika et al., 2014). In thyasirids such assays are challenging due to the difficulty in replicating their habitat in the laboratory for prolonged periods of time, especially because it is unfeasible to regulate the densities of free-living and symbiotic bacteria. Respiration measurements of starved individuals would yield information related to somatic maintenance, but these measurements would also reflect other processes such as maturity maintenance, and for symbiotic individuals they would also include symbiont consumption. To overcome these limitations, we suggest respiration studies conducted at different temperatures (like those performed in *Thyasira gouldi* by Blacknell, 1973), which would enable the estimation of the Arrhenius temperature, and would provide insight on the variation of the metabolic rate with temperature.

4.3. Growth and life history strategies

The assimilation rate and the somatic maintenance, together with the resource density, determine the growth rate of the individual (Table 1). For ad libitum food, a low assimilation rate and a low somatic maintenance in *T.* cf. *gouldi* are consistent with a lower growth rate relative to *Parathyasira*. This is evident in the slower development of *T.* cf. *gouldi*, and likely corresponds to a divergent reproductive strategy: all the maturity thresholds are reached later with respect to *Parathyasira*, and symbiotic *T.* cf. *gouldi* produces fewer, larger embryos, each with a greater amount of reserve energy (Table 7, Fig. 6). The cumulative energy invested in maturity is generally linked to gonad tissue, but in thyasirids the gonads are intermixed with the digestive gland, which precludes the use of traditional measurements (i.e. the gonadosomatic index). Future investigations should instead focus on determining egg and embryo sizes, fecundity as a function of length, and whether there is a correlation with seasonal changes.

Regardless of their differences in timing or energy requirements, *T.* cf. *gouldi* and *Parathyasira* show an extended stage before metamorphosis. A prolonged development agrees with the described ontogeny of the closest extant relatives of both species: *P. equalis* is characterized by an extended lecithotrophic development (i.e. a non-feeding larva that depends on the egg's reserves; Ockelmann, 1958); whereas *T. gouldi* has a lecithotrophic development, albeit benthic and direct (i.e. juveniles hatch from the egg; Blacknell and Ansell, 1974). It is noteworthy that this ontogenetic pattern may indicate that hatching from the egg occurs before birth as defined in DEB theory, because juveniles are not likely to feed immediately after hatching. Therefore, it would be relevant to further characterize the ontogenetic development of both species.

5. Conclusions

Our results suggest the mechanisms underlying two alternative evolutionary strategies for a thyasirid bivalve in an environment with seasonal forcing: for *T.* cf. *gouldi*, the bacterial symbionts may constitute an adaptation to buffer fluctuating resources by providing sustained nutrition to the host, which leads to an increase in the allocation flux towards maturation or reproduction. Conversely, the asymbiotic *Parathyasira* feeds on a seasonal resource, builds a comparatively larger energy reserve and has a faster life cycle with greater maintenance costs. These findings are likely to reflect a plausible role of the chemosymbiotic bacteria in the ecophysiology of the bivalve host, and highlight how the symbiotic association may alter the energy budget of a mixotrophic thyasirid.

Our findings are conditioned by the data that we used in the parameter estimation, which bound the species to the same puberty and ultimate sizes, in addition to an equal life span and reproductive output. These measurements are limited by low sample sizes and by anatomical characteristics of the thyasirids, which hinder the precision of our inference. However, our results indicate priority areas for future experiments to test the predictions of the model, and to further resolve the differences between symbiotic and asymbiotic thyasirids, particularly with respect to their reproductive biology. It would also be valuable to assess thyasirids from other regions to verify that the patterns in the data and in our estimation hold for populations outside of Bonne Bay. Our parameter estimates could be used to gain insight into the dynamics of resource availability and their relationship with the energy reserves, or to explore the consequences of the thyasirids' energy budget at the population and community levels.

Acknowledgements

We thank the staff of the Bonne Bay Marine Station for assistance

during sampling. Alison Pye and Rachelle Dove helped with the weighing of the samples at the Stable Isotope Laboratory (CREAIT TERRA Facility, MUN). We further thank two anonymous reviewers, Michael Kearney (guest editor of this special issue), and members of the Theoretical Biology Laboratory at MUN for their constructive comments on the manuscript. SA was supported by the Norwegian Science Council (NFR 255295). SCD was supported by a Natural Science and Engineering Research Council of Canada (NSERC) Discovery Grant (2015–06548). AH acknowledges financial support from an NSERC Discovery Grant (2014–05413) and the President's Doctoral Student Investment Fund (Memorial University).

Appendix A. Supplementary data

Supplementary material to this article can be found online at https://doi.org/10.1016/j.seares.2018.07.015.

References

AmP, 2017. *Tridacna gigas*, version 2017/08/07. Accessed: 2018-01-16 http://www.bio.vu.nl/thb/deb/deblab/add_my_pet/entries_web/Tridacna_gigas/Tridacna_gigas_res.html

Augustine, S., 2017. Maturity as quantifier for physiological time. Phys. Life Rev. 20, 40–42. http://linkinghub.elsevier.com/retrieve/pii/S157106451730009X.

Ballesta-Artero, I., Augustine, S., Witboard, R., Carrol, M., van der Meer, J., 2018. Energetics of the extremely long-living bivalve *Arctica islandica* based on a Dynamic Energy Budget model. J. Sea Res (this issue).

Batstone, R.T., Laurich, J.R., Salvo, F., Dufour, S.C., 2014. Divergent chemosymbiosis-related characters in *Thyasira* cf. *gouldi* (Bivalvia: Thyasiridae). PLoS One 9 (3), 1–9.

Blacknell, W.M., 1973. Aspects of the biology of *Thyasira gouldi* (Philippi) and its copepod parasite *Axinophilus thyasirae* (Bresciani and Ockelmann). PhD Thesis. University of Stirling.

Blacknell, W.M., Ansell, A.D., 1974. The direct development of Bivalve *Thyasira gouldi* (Phillipi). Thallasia Jugosl 10 (1/2), 23–43.

Dando, P.R., Spiro, B., 1993. Varying nutritional dependence of the thyasirid bivalves *Thyasira sarsi* and *T. equalis* on chemoautotrophic symbiotic bacteria, demonstrated by isotope ratios of tissue carbon and shell carbonate. Mar. Ecol. Prog. Ser. 92 (1–2), 151–158.

Dubilier, N., Bergin, C., Lott, C., 2008. Symbiotic diversity in marine animals: the art of harnessing chemosynthesis. Nature reviews. Microbiology 6 (10), 725–740. http://www.ncbi.nlm.nih.gov/pubmed/18794911.

Dufour, S.C., 2005. Gill anatomy and the evolution of symbiosis in the bivalve family Thyasiridae. Biol. Bull. 208 (3), 200–212.

Dufour, S.C., 2017. No Title. (Personal Communication).

Dufour, S.C., Felbeck, H., 2003. Sulphide mining by the superextensile foot of symbiotic thyasirid bivalves. Nature 426, 65–67.

Dufour, S.C., Laurich, J.R., Batstone, R.T., McCuaig, B., Elliott, A., Poduska, K.M., 2014. Magnetosome-containing bacteria living as symbionts of bivalves. ISME J. 8 (12), 2453–2462. https://doi.org/10.1038/ismej.2014.93.

Giolland, M., Dufour, S.C., 2015. Identification de bivalves de la famille des Thyasiridés formant un complexe d'espèces cryptiques dans un fjord de Terre-Neuve (Canada). (Unpublished).

Kooi, B.W., Troost, T.A., 2006. Advantage of storage in a fluctuating environment. Theor. Popul. Biol. 70 (4), 527–541.

Kooijman, S.A.L.M., 2010. Dynamic Energy Budget Theory for Metabolic Organisation, 3rd ed. Cambridge University Press, Cambridge. http://www.pubmedcentral.nih.gov/articlerender.fcgi?artid=2981979{&}tool=pmcentrez{&}rendertype=abstract.

Kooijman, S.A.L.M., 2013. Waste to hurry: dynamic energy budgets explain the need of wasting to fully exploit blooming resources. Oikos 122 (3), 348–357.

Kooijman, S.A.L.M., 2014. Metabolic acceleration in animal ontogeny: an evolutionary perspective. J. Sea Res. 94, 128–137. https://doi.org/10.1016/j.seares.2014.06.005.

Laurich, J.R., Batstone, R.T., Dufour, S.C., 2015. Temporal variation in chemoautotrophic symbiont abundance in the thyasirid bivalve *Thyasira* cf. *gouldi*. Mar. Biol. 162 (10), 2017–2028.

Lika, K., Kearney, M.R., Freitas, V., van der Veer, H.W., van der Meer, J., Wijsman, J.W.M., Pecquerie, L., Kooijman, S.A.L.M., 2011a. The "covariation method" for estimating the parameters of the standard Dynamic Energy Budget model I: philosophy and approach. J. Sea Res. 66 (4), 270–277. https://doi.org/10.1016/j.seares.2011.07.010.

Lika, K., Kearney, M.R., Kooijman, S.A.L.M., 2011b. The "covariation method" for estimating the parameters of the standard Dynamic Energy Budget model II: properties and preliminary patterns. J. Sea Res. 66 (4), 278–288. https://doi.org/10.1016/j.seares.2011.09.004.

Lika, K., Augustine, S., Pecquerie, L., Kooijman, S.A.L.M., 2014. The bijection from data to parameter space with the standard DEB model quantifies the supply-demand spectrum. J. Theor. Biol. 354, 35–47. https://doi.org/10.1016/j.jtbi.2014.03.025.

Marques, G., Augustine, S., Lika, K., Pecquerie, L., Domingos, T., Kooijman, S.A.L.M., 2018a. The amp project: comparing species on the basis of Dynamic Energy Budget parameters. PLoS Comput. Biol. 14 (5), e1006100. https://doi.org/10.1371/journal.pcbi.1006100.

Marques, G., Lika, K., Augustine, S., Pecquerie, L.T., Kooijman, S.A.L.M., 2018b. Fitting multiple models to multiple data. J. Sea Res. https://doi.org/10.1016/j.seares.2018.07.004. (this issue).

Ockelmann, W.K., 1958. The zoology of East Greenland: marine Lamellibranchiata. Medd. Grønland 18, 1–256.

Roeselers, G., Newton, I.L.G., 2012. On the evolutionary ecology of symbioses between chemosynthetic bacteria and bivalves. Appl. Microbiol. Biotechnol. 94 (1), 1–10.

Rohatgi, A., 2017. WebPlotDigitizer 4.0. Accessed: 2017-06-10 https://automeris.io/WebPlotDigitizer

Southward, E.C., 1986. Gill symbionts in thyasirids and other bivalve molluscs. J. Mar. Biol. Assoc. U. K. 66, 889–914.

Taylor, J.D., Glover, E.A., 2010. Chemosymbiotic Bivalves. In: Kiel, S. (Ed.), The Vent and Seep Biota. vol. 33. Springer, Netherlands, pp. 107–135. Ch. 5. https://doi.org/10.1007/978-90-481-9572-5.

Taylor, J.D., Williams, S.T., Glover, E.A., 2007. Evolutionary relationships of the bivalve family Thyasiridae (Mollusca: Bivalvia), monophyly and superfamily status. J. Mar. Biol. Assoc. UK 87 (02), 565–574. https://doi.org/10.1017/S0025315407054409.

The MathWorks Inc, 2017. MATLAB Release 2017a.

Zanzerl, H., Dufour, S.C., 2017. The burrowing behaviour of symbiotic and asymbiotic thyasirid bivalves. J. Conchol. 42 (5), 299–308.